Environmental Science
Water Research & Technology

ROYAL SOCIETY OF CHEMISTRY

PAPER

View Article Online
View Journal | View Issue

Cite this: *Environ. Sci.: Water Res. Technol.*, 2021, **7**, 222

Simple preparation method for Styrofoam–TiO_2 composites and their photocatalytic application for dye oxidation and Cr(VI) reduction in industrial wastewater†

Youn-Jun Lee,[a] Chang-Gu Lee, *[a] Jin-Kyu Kang,[b] Seong-Jik Park[c] and Pedro J. J. Alvarez [d]

Received 26th August 2020,
Accepted 23rd November 2020

DOI: 10.1039/d0ew00787k

rsc.li/es-water

This study investigates a simple method for the preparation of floating photocatalysts in which the surface of expanded polystyrene (EPS) is partially dissolved using a diluted solvent that contains TiO_2 particles. The acetone volume content (v/v) and TiO_2 weight content (w/v) of the diluted solvent and the stirring time of the diluted solvent and EPS were optimized through methylene blue (MB) oxidation experiments. The surface morphology, TiO_2 weight ratio, and functional group of the EPS–TiO_2 composite (TiEPS) were characterized. Ethyl acetate, benzene, and acetone were selected as suitable solvents for dilution using this simple preparation method. MB degradation efficiency of the TiEPS remained stable over 20 reuse cycles, and minimal TiO_2 leaching was observed (up to 3.6 μg L^{-1} of titanium). Photocatalytic reduction of Cr(VI) in wastewater from a plating plant was evaluated *via* a composite prepared using waste expanded polystyrene (W-TiEPS). More than 99% of the Cr(VI) was reduced to Cr(III) within 75 min by W-TiEPS amended with citric acid under UV-A irradiation (λ_{max} = 350 nm, 3.93 × 10^{-9} einstein per cm^2 s^{-1}). These results suggest that the floating photocatalyst produced *via* this simple and scalable method should be considered to remove Cr(VI) and perhaps other water and wastewater contaminants.

Water impact

A novel and facile preparation method for a floating photocatalyst is described, using a diluted solvent to modify only the surface of the EPS and to immobilize TiO_2. The prepared photocatalyst composite exhibited high and stable activity in photocatalytic oxidation and photocatalytic reduction of contaminants in water. This method is expected to contribute to the scale up of floating photocatalysts and recycling of waste Styrofoam.

1. Introduction

Since photoelectrochemical water splitting was first reported by Fujishima and Honda in 1972,[1] extensive research has been conducted in the field of photocatalytic water treatment.[2–5] Advanced photocatalytic oxidation processes (AOPs) are considered environmentally friendly water treatment technologies because no precursor chemical oxidizing agents such as O_3 and H_2O_2 are required to destroy the water contaminants, unlike conventional AOPs.[6] Photocatalysis can also be applied to the photocatalytic reduction of metal compounds in water alongside the photocatalytic oxidation of organic molecules.[7,8]

In photocatalytic water treatment, the photocatalyst may be immobilized onto the surface of a substrate to avoid the need for an energy-intensive separation process such as membrane filtration for recovering the catalyst.[9–11] A suitable support material such as a floating photocatalyst can maximize light harvesting while also facilitating oxidation due to the proximity of the air/water interface.[12,13] Such materials can also be easily recovered from the water surface after treatment.[14] Various lightweight substrates such as perlite, vermiculite, glass microbeads, expanded graphite, cork, and polymers have been used to fabricate floating photocatalysts.[14–20]

Expanded polystyrene (EPS), commonly referred to as "Styrofoam", is a lightweight, inexpensive, and readily available material that has good insulation properties and high chemical and mechanical stability.[12,21–24] EPS has therefore been widely

[a] *Department of Environmental and Safety Engineering, Ajou University, Suwon 16499, Republic of Korea. E-mail: changgu@ajou.ac.kr; Tel: +82 31 219 2405*
[b] *Environmental Functional Materials and Water Treatment Laboratory, Seoul National University, Seoul, Republic of Korea*
[c] *Department of Bioresources and Rural System Engineering, Hankyong National University, Anseong, Republic of Korea*
[d] *Department of Civil and Environmental Engineering, Rice University, Houston, TX 77005, USA*

† Electronic supplementary information (ESI) available. See DOI: 10.1039/d0ew00787k

used in a number of applications such as buildings and construction, industrial packaging, food containers, and fishing net floats.[22,25,26] However, it does not decompose in the natural environment because of its inert nature, and the discharge of large amounts of EPS byproducts can lead to a serious environmental problem known as "white pollution".[13,23] Accordingly, EPS-supported floating photocatalysts offer an opportunity to recycle waste Styrofoam.

Several studies have been conducted on the preparation and photocatalytic properties of TiO_2-immobilized EPS composites. Altın and Sökmen[23] conducted a thermal attachment process to anchor anatase TiO_2 nanoparticles (with a particle size of 44 nm) onto PS beads. The photocatalytic properties of the produced material were tested for the removal of methylene blue (MB) and reductive removal of Cr(VI) as model contaminants. Magalhães and Lago[12] reported the simple preparation of a floating photocatalyst based on TiO_2 grafted onto EPS by spraying a PS solution; the floating photocatalyst produced showed high efficiency in dye degradation. Varnagiris *et al.*[27] deposited a photoactive anatase TiO_2 film onto the surface of EPS using a reactive pulsed DC magnetron sputtering technique. The photocatalytic properties were investigated by bleaching the MB solution under UV irradiation. However, to the best of our knowledge, the simple approach of partially dissolving the surface of EPS using diluted solvent that contains TiO_2 has never been used to immobilize TiO_2 onto EPS surfaces.

In this study, this simple approach of using diluted solvents was tested for TiO_2 immobilization on the surface of EPS. The effects of solvent volume content, TiO_2 weight content, and stirring time were evaluated using a photocatalytic dye decomposition test. The photocatalytic activity of EPS–TiO_2 composites prepared using different diluted solvents and the reusability of the prepared photocatalyst were analyzed. The photocatalyst prepared using waste EPS was evaluated in photocatalytic reduction tests to remove Cr(VI) in plating wastewater, and the effects of sacrificial organic compounds (*i.e.*, electron donors) were also examined.

2. Materials and methods

2.1 Materials

EPS beads were obtained from the Edu Store (Seoul, Korea). The discarded expanded polystyrene was obtained from the beach at Buan, Korea. A wastewater sample containing 844.2 mg L^{-1} of Cr(VI) was obtained from a local plating plant (Ansan, Korea) (Table S1†). The methylene blue (MB) ($C_{16}H_{18}ClN_3S$, ≥96%), citric acid monohydrate ($C_6H_8O_7{\cdot}H_2O$, ≥99.5%), oxalic acid dihydrate ($C_2H_2O_4{\cdot}2H_2O$, ≥99%), 0.05 mol L^{-1} EDTA disodium salt solution ($C_{10}H_{14}N_2Na_2O_8$), methyl alcohol (CH_3OH, ≥99.5%), isopropyl alcohol (IPA, C_3H_8O, ≥99.5%), ethyl acetate (EA, $C_4H_8O_2$, ≥99.7%), benzene (C_6H_6, ≥99.5%), acetone (C_3H_6O, ≥99%), and potassium chloride solution (KCl, 3.3 M) were purchased from Samchun Pure Chemical Co. Ltd (Pyeongtaek, Korea). The titanium dioxide (P25) (TiO_2, ≥99.5%) was purchased from Sigma-Aldrich Co., Ltd. (St. Louis, USA) and the ethyl alcohol (C_2H_5OH, ≥99.5%) was purchased from Duksan Pure Chemicals Co., Ltd. (Ansan, Korea). Deionized water (DI) with a resistivity of 18.2 MΩ cm^{-1} was purified using a Direct-Q 3 UV system (Millipore, USA).

2.2 Synthesis of the EPS–TiO_2 composites

EPS–TiO_2 (TiEPS) was prepared by dissolving the surface of the EPS. Typically, 0.8 g of TiO_2 nanoparticles were sonicated (Power sonic 420, Hwashin, Korea) in a 10%, 20 mL acetone solution for 1 h, after which 0.15 g expanded polystyrene beads with a diameter of 2–3 mm were added to the above solution. After stirring for 30 min, the TiO_2-immobilized EPS beads were separated and dried at room temperature for 24 h. The dried TiO_2-immobilized EPS beads were stirred vigorously in 500 mL DI for 4 h to remove any weakly attached TiO_2 particles. The washed TiO_2-immobilized EPS beads were then dried overnight in a vacuum oven (FTVO-701, SCI FINETECH Co., Korea) at 80 °C. The TiO_2 weight ratio, solvent concentration, anchoring reaction time, and amount of dissolving solvent used were varied in order to achieve the optimal MB degradation.

A modified immobilization method was used to synthesize the EPS–TiO_2 composite with waste EPS (W-TiEPS) (Fig. S1†). EPS waste particles of between 2 mm and 5 mm were separated using a sieving process. The separated EPS particles were washed with tap water, ethanol, and DI and dried overnight in a convection oven at 70 °C (OF-22GW, JEIO TECH, Korea). Afterwards, 1.875 g of the dried EPS waste was added to a 10% acetone and 4% TiO_2 solution (250 mL) and mixed in a shaking incubator (SJ-808SF, SEJONG SCIENTIFIC CO, Korea) at 140 rpm to synthesize W-TiEPS. The W-TiEPS particles were recovered and dried at room temperature for 48 h. After drying, the W-TiEPS particles were sonicated for 10 min and stirred vigorously in 1 L DI for 4 h. The washed W-TiEPS particles were then dried overnight in a convection oven at 70 °C for the Cr(VI) photoreduction experiments.

2.3 EPS–TiO_2 characterization

Surface morphology and elemental mapping were observed using a field emission scanning electron microscope/energy dispersive spectrometer (FE-SEM/EDS) (JSM-6700F, JEOL, Japan). The X-ray diffraction (XRD) of samples was determined using X-ray diffractometer (Rigaku D/max-2500 V/PC diffractometer, Rigaku, Japan). The surface functional groups of the TiEPS were measured by Fourier transform infrared-attenuated total reflectance (FTIR-ATR) spectroscopy (Nicolet iS50, Thermo, Massachusetts, USA). The weight fraction of the immobilized TiO_2 on the TiEPS was analyzed by thermogravimetric analysis (TGA) (Pyris 1, Perkin Elmer, Massachusetts, USA). Eluted Ti(IV) ions were detected in the solution after the MB photocatalysis experiment using an inductively coupled plasma–mass spectrometer (ICP-MS) (7700x ICP-MS, Agilent Technology, California, USA). Cations and anions were detected in the

wastewater using ICP-OES (Optima 8300, Perkin Elmer Massachusetts, USA) and ion chromatography (Dionex Aquion, Thermo, Massachusetts, USA).

2.4 Photocatalytic degradation experiments

The photocatalytic activities of TiEPS and W-TiEPS were investigated *via* the oxidation of methylene blue and the reduction of Cr(VI), separately. Six UV lamps (4 W) that were placed in a black acrylic box were used as a UV-A light source (λ_{max} = 350 nm). A quartz reactor was positioned at the center of the acrylic box, 6 cm from the lamps. The light reaching the quartz reactor was determined by ferrioxalate actinometry as 3.93×10^{-9} einstein per cm^2 s^{-1}. Except when otherwise mentioned, solutions comprising 5 μM MB and wastewater that had been diluted 100 times (8.442 mg L^{-1} Cr(VI)) were used for the experiments, with 0.08 g of TiEPS and 0.1 g of W-TiEPS added to 50 mL of a solution. Reusability tests carried out on the TiEPS and W-TiEPS were performed for 3 h and 1.5 h, respectively. The pH of the chromium wastewater solution was adjusted to 2.0, 5,0, 8.0 by adding 1 M HCl or 1 M NaOH and measured with a pH meter (Orin Star A211, Thermo, Massachusetts, USA). The ionic strength of solution was adjusted by KCl.

The residual MB concentration was analyzed using a UV/visible spectrophotometer (NEO-S2117, NEOGEN, Korea) at a wavelength of 664 nm. The concentration of hexavalent chromium was determined by the diphenyl carbazide colorimetric method using a UV/visible spectrophotometer at 540 nm. The dissolved organic carbon (DOC) and metals in the wastewater sample were measured using a TOC analyzer (TOC-VCSH, Shimadzu, Kyoto, Japan) and inductively coupled plasma-optical emission spectroscopy (ICP-OES, Optima 8300, Perkin-Elmer, USA), respectively.

All experiments were replicated and one tailed *t*-test was used to determine statistically significant differences between treatments at the 95% confidence level ($p < 0.05$).

3. Results and discussion

3.1 Simple preparation method for EPS–TiO_2 floating photocatalysts

Acetone is the most widely used solvent in industry and has a relatively low toxicity compared to many other industrial solvents.[28] Unlike benzene and ethyl acetate, which are good solvents, acetone is a poor solvent for PS but is completely miscible with water.[28–30] We found that acetone can dissolve some surface EPS and immobilize TiO_2 particles when diluted with water (Scheme 1). The surface of the EPS was plasticized by the solvent to enable impregnation of the TiO_2 particles.[31] Pristine EPS balls were 3.19 ± 0.33 mm in diameter and did not exhibit any photocatalytic activity. The diameter of the balls decreased slightly to 3.08 ± 0.35 mm when they were reacted with a diluted solvent containing 10% (v/v) acetone and 4% (w/v) TiO_2, after which they became floating photocatalysts (Fig. S2†). With the TiO_2 dose fixed at 4% (w/v), the TiEPS balls were observed to gradually decrease to 2.84 ± 0.35 mm, 2.83 ± 0.38 mm, 2.54 ± 0.30 mm, and 1.52 ± 0.22 mm in diameter as the acetone volume content (v/v) was increased to 30%, 50%, 70%, and 90%, respectively. EPS balls were completely dissolved in undiluted acetone containing 4% TiO_2, and the TiO_2 particles could not be fixed.

To optimize the simple method used to prepare TiEPS, the effects of acetone volume content (v/v) and TiO_2 weight content (w/v) in the diluted solvent and the time allowed for stirring with diluted solvent were evaluated in terms of photocatalytic activity. As shown in Fig. 1(a), the photocatalytic activity per unit mass of TiEPS decreased as the volume content (v/v) of acetone was increased at a constant TiO_2 weight content (4%, w/v). This is because the mass of fixed TiO_2 particles increased slightly per unit mass of EPS as the volume of acetone increased, but the spacing between the TiO_2 particles decreased and they aggregated as the diameter of the composites decreased. Aggregation of TiO_2 particles is known to decrease photocatalytic activity.[32,33] Similar results were found in experiments varying

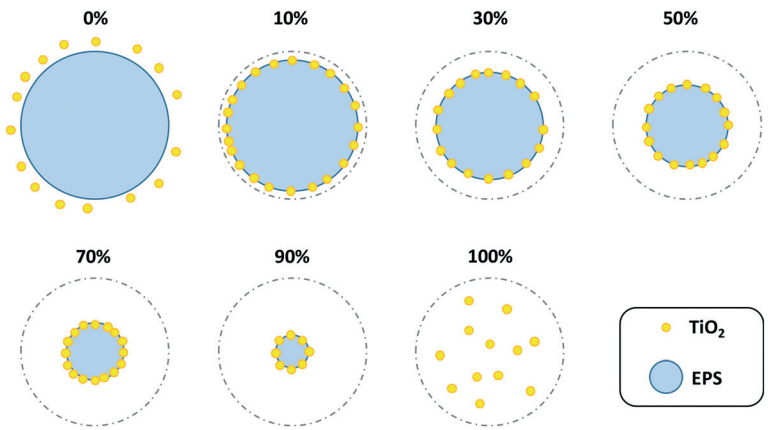

Scheme 1 Schematic diagram of the simple method of preparing EPS–TiO_2 composites using diluted solvents. Volume contents of solvent (v/v): 0, 10, 30, 50, 70, 90, and 100%.

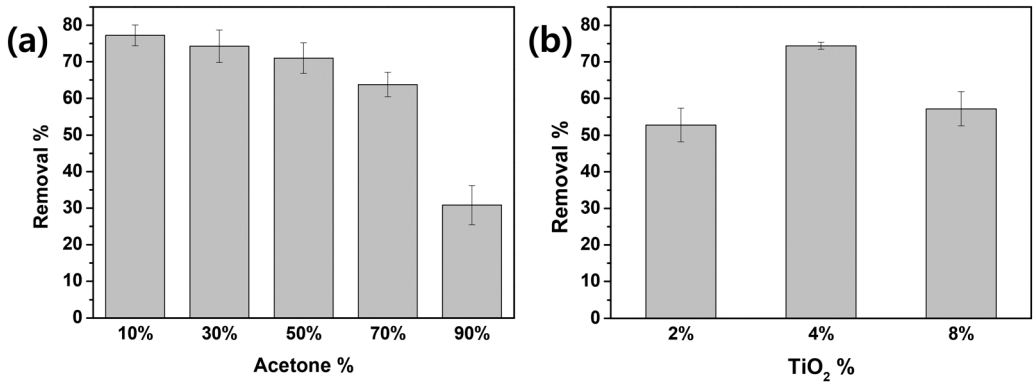

Fig. 1 Effect of (a) acetone volume content (v/v) and (b) TiO_2 weight content (w/v) in a diluted solvent on the photocatalytic activity of EPS–TiO_2 composites. Photocatalytic experimental conditions: initial dye concentration = 5 μM; catalyst dose: 1.6 g L^{-1}; irradiation time = 60 min; light intensity = 3.93×10^{-9} einstein per cm^2 s^{-1}. Data are plotted as mean of replicates and error bars represent range of observed values.

the TiO_2 weight content (w/v) with a fixed acetone volume (10%, v/v) (Fig. 1(b)). The photocatalytic activity of the TiEPS increased as the TiO_2 weight content (w/v) increased from 2% to 4%, but the treatment efficiency decreased with further addition of TiO_2 (8%, w/v). This is likely due to excess amounts of photocatalyst hindering light penetration.[34]

The effect of the stirring time on the photocatalytic activity in diluted solvent containing 10% (v/v) acetone, 4% (w/v) TiO_2, and the EPS balls was negligible (Fig. S3†). The preparation conditions of TiEPS were optimized based on the results of the photocatalytic degradation, and a stirring period of 30 min with a diluted solvent containing 10% (v/v) acetone and 4% (w/v) TiO_2 were selected as the optical conditions.

3.2 Characteristics of the EPS–TiO_2 floating photocatalyst

The surface morphology of the prepared EPS–TiO_2 floating photocatalyst was observed by FE-SEM. The spherical shape of the EPS was maintained by the diluted solvent and the immobilized TiO_2 particles during the disruption of the surface (Fig. 2 and S4†). However, the surface of the TiEPS was rougher than that of the pristine EPS balls. Based on the associated EDS analysis, the surface components of the pristine EPS balls were carbon (C) and oxygen (O) (Fig. S5†), while the surface components of the TiEPS were carbon (C), oxygen (O), and titanium (Ti) (Fig. 3 and S6†), indicating that the TiO_2 particles were successfully fixed onto the surface of the EPS balls. In addition, EDS mapping confirmed that the fixed TiO_2 particles were uniformly distributed on the surface of the EPS balls.

The mass of TiO_2 particles immobilized on the surface of the EPS balls was calculated by TGA analysis (Fig. 4(a)). The pristine EPS balls began to decompose at 175.38 °C, with residues of less than 0.70% (w/w) at 610.98 °C. The thermal decomposition properties of the pristine balls were similar to those reported in the literature,[35,36] with a $T_{50\%}$ (50% weight loss temperature) of 403.05 °C. The mass loss of the sample prepared with dilute solvents containing 10% (v/v) acetone and 4% (w/v) TiO_2 suggested that 8.06% (w/w) TiO_2 was immobilized on the EPS–TiO_2 composite. As described previously, the mass of the fixed TiO_2 increased to 10.65% (w/w) as the volume of acetone reached 90% (v/v) (Fig. S7†). The $T_{50\%}$ values of the samples prepared using 10% and 90% acetone increased to 410.14 °C and 422.75 °C, respectively,

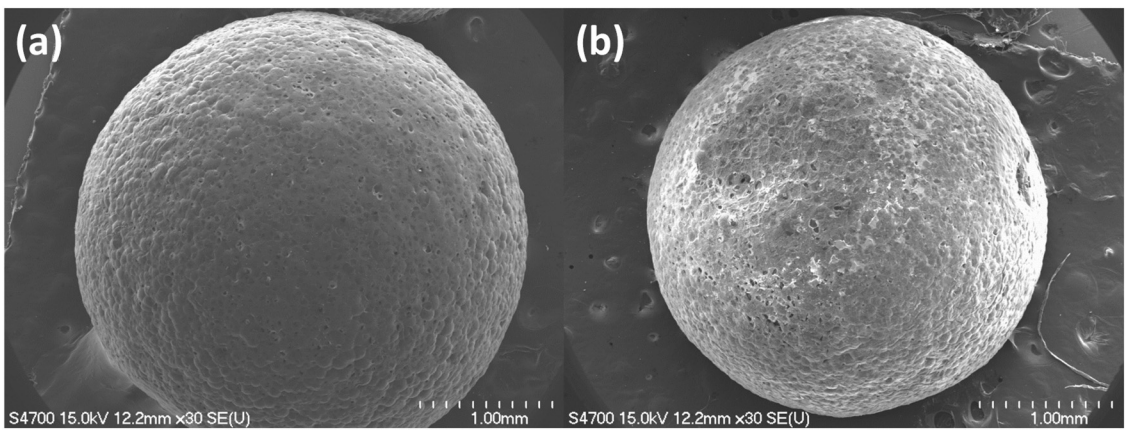

Fig. 2 FE-SEM images (×30) of (a) pristine EPS ball and (b) EPS–TiO_2 composite prepared using a diluted solvent containing 10% (v/v) acetone and 4% (w/v) TiO_2.

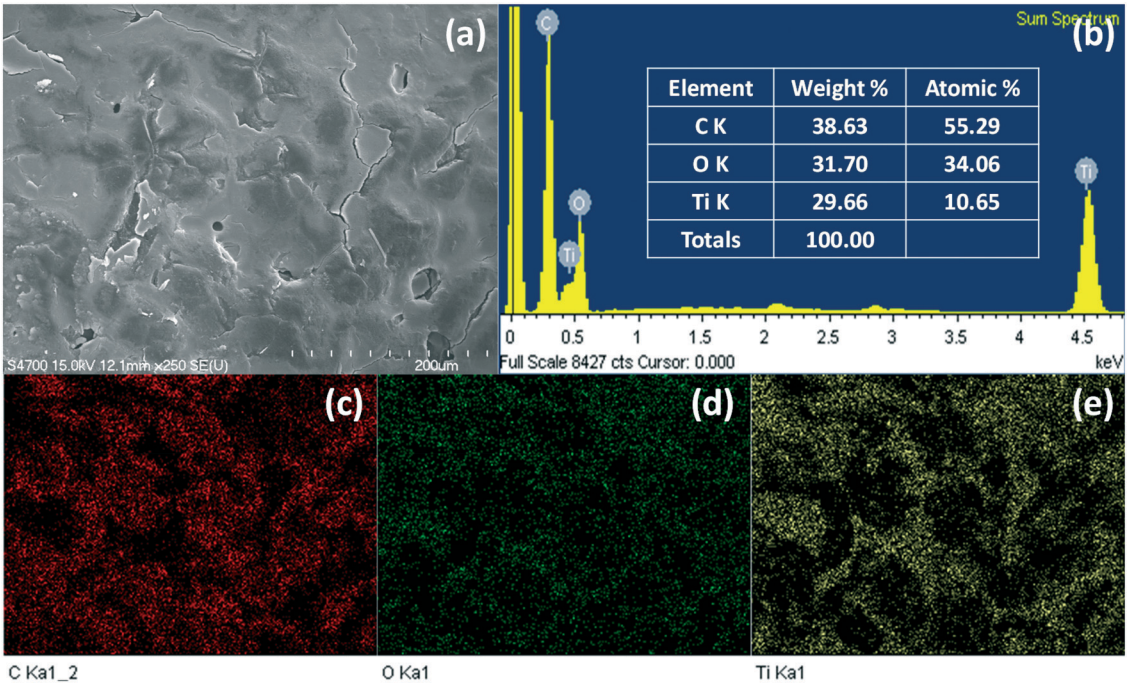

Fig. 3 EPS–TiO_2 composite prepared using a diluted solvent containing 10% (v/v) acetone and 4% (w/v) TiO_2: (a) surface SEM image (×250), (b) elemental analysis by EDS, and EDS mappings of (c) C, (d) O, and (e) Ti.

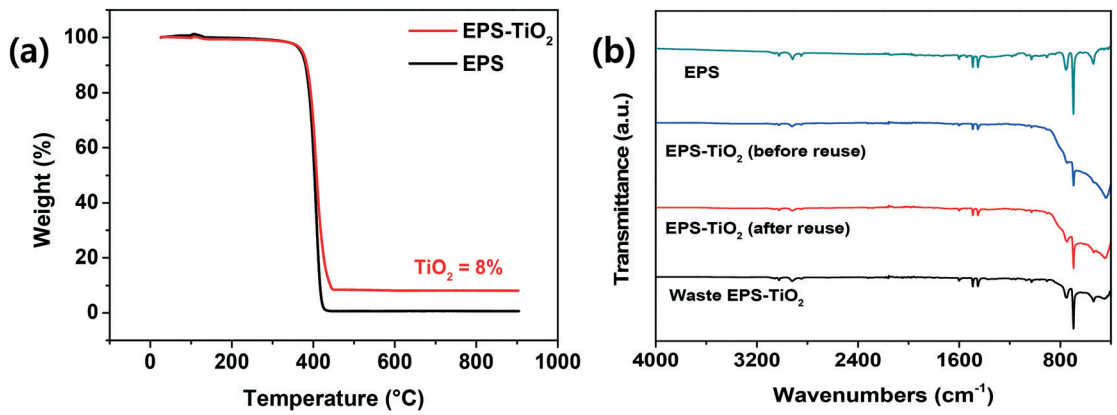

Fig. 4 (a) TGA and (b) FTIR analyses of pristine EPS balls and EPS–TiO_2 composites prepared using a diluted solvent containing 10% (v/v) acetone and 4% (w/v) TiO_2.

due to the incorporation of nanoparticles into the polymer composite, thus enhancing the thermal stability.[9,36]

To demonstrate the successful binding of TiO_2 particles, an XRD analyses of EPS–TiO_2 and EPS were performed (Fig. S8†). The broad 2θ diffraction peak around 21° was ascribed to polystyrene,[37] while the typical diffraction peaks of anatase appeared in EPS–TiO_2 floating photocatalyst at 2θ = 25.29°, 36.91°, 37.73°, 38.54°, 48.02°, 53.81°, and 55.04° (JCPDS 00-021-1272).[38] Weak anatase diffraction peaks indicate uniformly dispersed TiO_2 particles on the EPS surface.[37]

The functional groups on the TiEPS were studied using FTIR spectroscopy (Fig. 4(b)). Pristine EPS balls displayed the typical FTIR spectra of Styrofoam as a common material.[39–42] The peaks observed at 3059, 3025, 2917 and 2849 cm^{-1} were due to the stretching and bending vibrations of the C–H bonds. The peaks at 1601 and 1583 cm^{-1} confirm the C=C stretching. The peaks at 1492, 1452, 1028, 907, 843, 756, and 697 cm^{-1} were assigned to the C–H vibrations of the phenyl groups. The adsorption peak at 1067 cm^{-1} was attributed to C–O bond stretching. The functional groups of the Styrofoam were not changed by TiO_2 immobilization when a diluted solvent was used, and the broad band lying below 800 cm^{-1} that was associated with TiEPS was assigned to the bending vibrations of Ti–O–Ti.[43,44]

3.3 Evaluation of photocatalytic performance and reusability

The photocatalytic performance of the EPS–TiO_2 floating photocatalyst was evaluated by model dye (MB) degradation

with UV irradiation (Fig. 5). The adsorption of dye onto both pristine EPS and TiEPS under dark conditions was negligible. The dye concentration also did not change when UV was used alone (photolysis) or when UV was applied to pristine EPS. Thus, the degradation of MB by TiEPS under UV irradiation was clearly due to the photocatalytic reaction (Fig. 5(a)). The apparent first-order degradation kinetic constant (k_{app}) of the MB that resulted from the photocatalytic reaction of TiEPS was 0.042 ± 0.006/min, which is comparable to the values (0.006–0.029/min) reported in the literature.[14,45,46] Nevertheless, more reaction times are required to achieve mineralization with TOC removal whereas the UV-vis spectrum of MB decreases rapidly (Fig. S9†). As mentioned previously, benzene and ethyl acetate are good solvents for PS and can also be used with this simple preparation method by diluting with ethanol. The EPS–TiO_2 floating photocatalysts prepared using ethanol containing 4% (w/v) TiO_2 with 20% (v/v) benzene and 30% (v/v) ethyl acetate exhibited similar photocatalytic performance (Fig. 5(b)). Nevertheless, these solvents require other solvents such as ethanol for dilution instead of water, which hinders their feasibility and poses environmental concerns.

The photocatalytic performance of the TiEPS was retained over 20 cycles (indiscernible from the initial value ($p < 0.05$)) and demonstrated excellent reusability (Fig. 6). Over these 20 cycles, there was no change in the rate of the MB degradation or the weight of the photocatalyst, which implies that the deformation of the TiEPS was negligible during continuous photocatalytic degradation. Furthermore, according to the ICP-MS analysis, only 3.6 μg L^{-1} (detection limit 1 μg L^{-1}) of titanium leached from the composite into the water during the photocatalytic degradation, which is similar to the concentration that is found naturally in water (approximately 0.7–43 μg L^{-1}).[47] In addition, the functional groups of TiEPS remained intact after 20 uses.

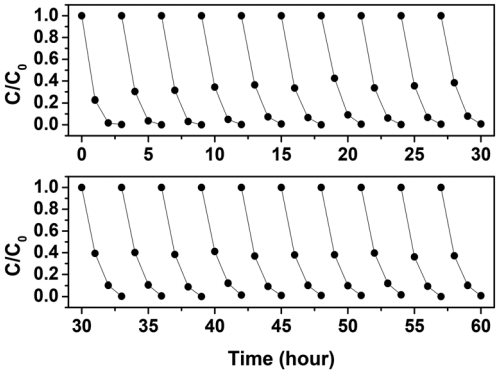

Fig. 6 Reuse of EPS–TiO_2 composite to remove methylene blue ($[MB]_0$ = 5 μM) over 20 cycles under UV irradiation (catalyst dose: 1.6 g L^{-1}; light intensity = 3.93×10^{-9} einstein per cm^2 s^{-1}).

3.4 Application to the photocatalytic reduction of Cr(VI) in plating wastewater

3.4.1 Effect of sacrificial compounds (electron donors) on Cr(VI) reduction. To assess the effect of the sacrificial compounds, which accelerate the photoreduction of Cr(VI) by hindering the electron–hole recombination, a certain amount (0.4 mM) of EDTA, oxalic acid, citric acid, isopropyl alcohol, or methanol were added to the photocatalytic reaction as scavenger agents (Fig. 7(a)). The photocatalytic Cr(VI) reduction was significantly enhanced in the presence of EDTA, oxalic acid, and citric acid under the experimental conditions used in this study. However, it has also been reported that the photocatalytic reduction of Cr(VI) can be hindered by EDTA and oxalic acid as a result of interference by the adsorbed organic molecules that have higher molecular size and adsorption efficiency for the surface of TiO_2 than Cr(VI).[48,49]

Citric acid is well known to promote Cr(VI) reduction by effectively scavenging the positive holes generated during the photocatalytic process owing to its electron-rich property.[50] Thus, citric acid was chosen as a sacrificial molecule, and the photoreduction of Cr(VI) was observed to accelerate as the citric acid concentration increased from 0.01 mM to 6.4 mM (Fig. 7(b)). By adding 0.4 mM citric acid, 8.442 mg L^{-1} Cr(VI) was completely removed within 75 min, and the electrical energy per order (EEO) value for the photocatalytic Cr(VI) reduction in real plating wastewater decreased from 2472 to 159 kW h m^{-3} under our experimental conditions.

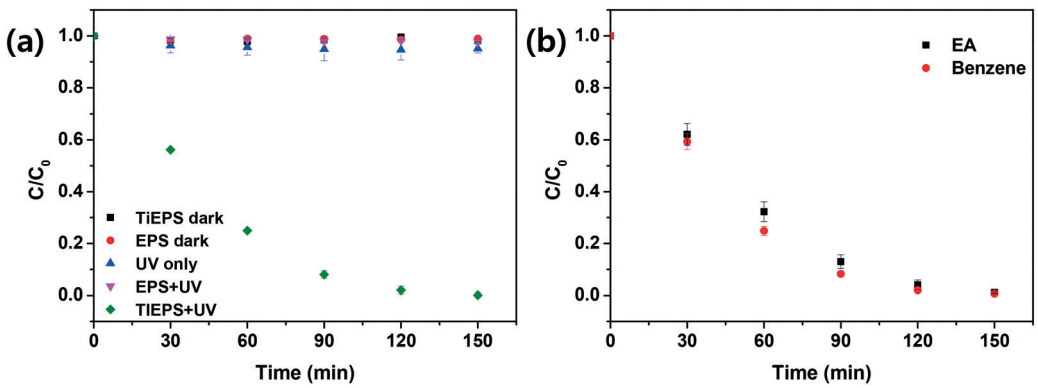

Fig. 5 Photocatalytic removal of methylene blue dye. Panel (a) shows negligible removal by adsorption under dark conditions or photolysis using UV. Panel (b) shows photocatalytic activity of EPS–TiO_2 composites prepared using different diluted solvents under UV irradiation. Photocatalytic experimental conditions: initial dye concentration = 5 μM; catalyst dose: 1.6 g L^{-1}; light intensity = 3.93×10^{-9} einstein per cm^2 s^{-1}. Data are plotted as mean of replicates and error bars represent range of observed values.

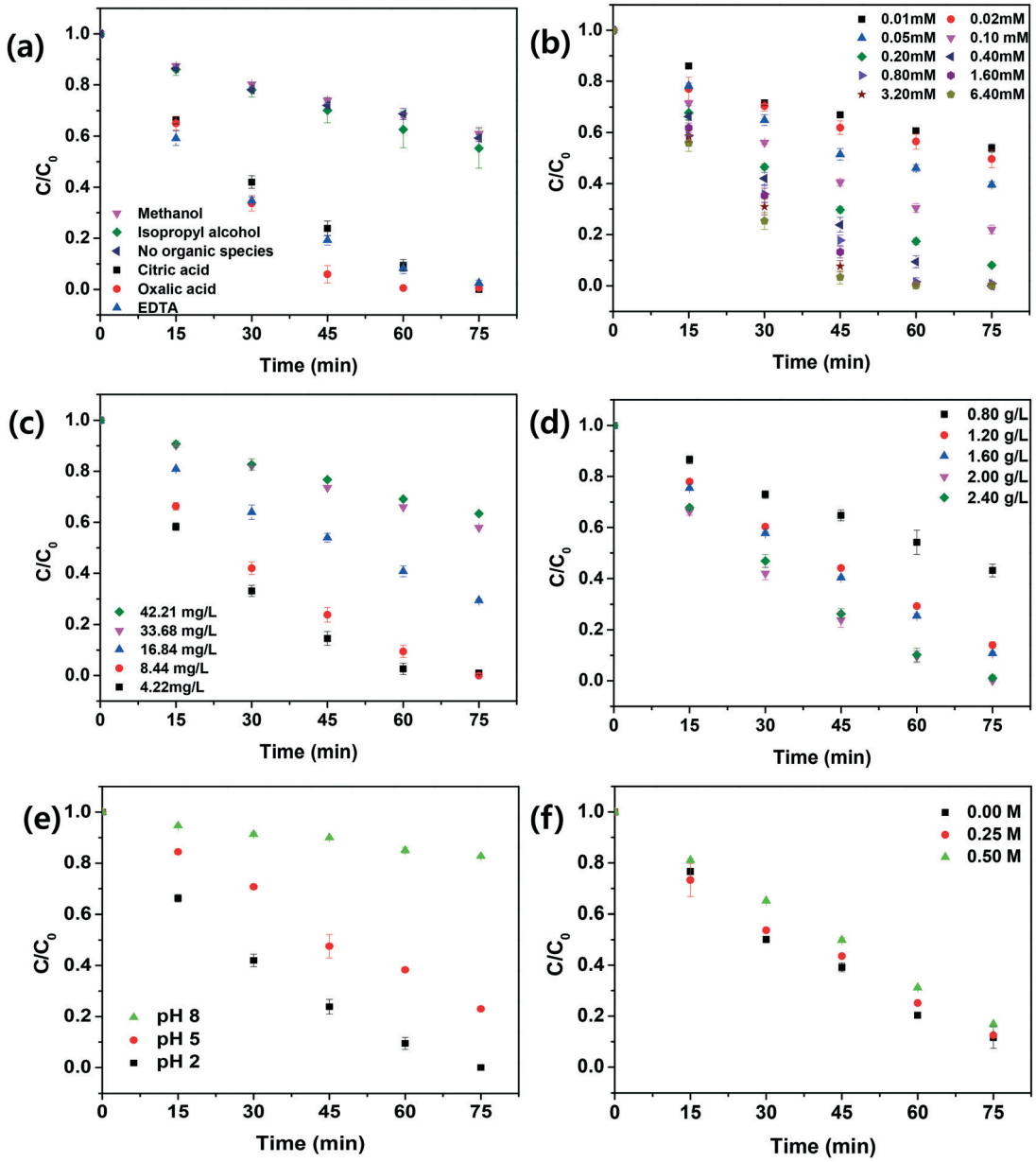

Fig. 7 Effects of (a) sacrificial compound types, (b) citric acid concentrations, (c) initial Cr(VI) concentrations, (d) catalyst dose, (e) solution pH, and (f) ionic strength on photocatalytic Cr(VI) reduction by W-TiEPS in industrial wastewater (light intensity = 3.93×10^{-9} einstein per cm^2 s^{-1}). Data are plotted as mean of replicates and error bars represent range of observed values.

The effect of isopropyl alcohol and methanol on the photocatalytic Cr(VI) reduction was negligible. The adsorption of these compounds to the TiO_2 surface occurs through weak hydrogen bonding, while the carboxyl groups of organic acids can form complexes with TiO_2 and are attached to the surface through strong chemical adsorption. Since the photocatalytic reduction of Cr(VI) mainly occurs on the surface of the catalyst, the scavenging agents that efficiently adsorbs on the TiO_2 surface are effective.[51] Cr(VI) was partially photoreduced under UV irradiation without the presence of photocatalyst, but was not reduced when placed in the dark with photocatalyst in the presence of citric acid (Fig. S10(a)†). This is because a lone electron pair on the hydroxyl group that is attached to the carboxyl group may become excited under UV irradiation and move into the empty d orbital of the Cr(VI), resulting in the reduction of Cr(VI) as the citric acid is depleted.[50] The Cr(III) concentration increased as the Cr(VI) concentration decreased (Fig. S11†). Since the experiment was carried out under acidic conditions (pH 2), the reduced chromium did not precipitate, and the total chromium concentration remained constant (11.63 ± 0.15 mg L^{-1}).

3.4.2 Effect of Cr(VI) concentration and catalyst dose. The effect of initial Cr(VI) concentration was also evaluated using a system with citric acid (molar ratio, [Cr(VI)]:[citric acid] = 1: 3.24) (Fig. 7(c)). The efficiency of the photocatalytic Cr(VI) reduction gradually decreased as the initial Cr(VI) concentration

was increased by ten-fold from 4.22 to 42.21 mg L^{-1}. The negative effect of a high initial concentration can be attributed to the saturation of the surface of the catalyst with Cr(VI) molecules and to the screening effect of the Cr(VI) species hindering light penetration and TiO_2 photoactivation.[49]

Photocatalytic Cr(VI) reduction efficiency increased as the amount of catalyst used was increased from 0.8 to 2.0 g L^{-1} (Fig. 7(d)), which can be attributed to the increase in the number of active sites available.[52] However, the change in the photocatalytic Cr(VI) reduction efficiency was negligible as the quantity of catalyst was increased from 2.0 to 2.4 g L^{-1}, and high amounts of catalyst that exceed the optimum conditions can hinder the access to light, resulting in poor activation of the photocatalyst.[7,8]

3.4.3 Effect of solution pH and ionic strength on Cr(VI) reduction. Solution pH is essential for Cr(VI) reduction as it dominates the existing species of Cr(VI) (H_2CrO_4, $HCrO_4^-$, and CrO_4^{2-}). Based on the visual MINTEQ 3.0 analysis (Fig. S12†), photocatalytic reduction of Cr(VI) was investigated at pH 2, 5, and 8 with photocatalyst dose at 2.0 g L^{-1} and initial Cr(VI) concentration of 8.44 mg L^{-1}. As shown in Fig. 7(e), the Cr(VI) reduction was decreased as the pH of the solution increased. The photoreduction efficiency of Cr(VI) decreased to 76.98 ± 0.88% and 17.38 ± 0.17% at pH 5 and 8, while Cr(VI) completely reduced at pH 2 during 75 min irradiation. The high reduction efficiency at pH 2 compared to others indicates that the acidic condition is more favorable for the Cr (VI) reduction.[50,53] On the contrary, the decrease in photoreduction with increasing pH could be attributed to the deposition of $Cr(OH)_3$, which lower the reduction efficiency by covering the surface of the photocatalyst and reduce the light penetration.[53,54]

The effect of ionic strength on Cr(VI) reduction was also evaluated (Fig. 7(f)). The photocatalytic reduction rate of Cr(VI) did not change significantly as the KCl concentration increased to 0.25 M and 0.50 M compared to the absence of KCl. These observations indicate that the ionic strength has no significant influence on the photocatalytic reduction of Cr(VI), which was in accordance with the previous studies.[54,55] The slight decrease in the reduction rate might be attributed to photocorrosion due to the specific adsorption of Cl^- on the photocatalyst.[50]

3.4.4 Reusability of the catalyst for Cr(VI) reduction in plating wastewater. A final important aspect to consider is the ability to reuse TiO_2-immobilized photocatalysts. Reuse of the photocatalyst would significantly reduce the cost of the photocatalytic operating system while also limiting the amount of solid waste generated.[49] W-TiEPS particles were reused for 5 consecutive photocatalytic reduction cycles under conditions of 8.44 mg L^{-1} Cr(VI), 0.4 mM citric acid, and 2.0 g L^{-1} of catalyst (Fig. S10(b)†). The photoreduction efficiency of the W-TiEPS composite continued to decrease with the number of reuses, decreasing by approximately 28% after five consecutive photoreduction cycles. The decrease in photoreduction activity during a reuse cycle can be attributed to the presence of residual intermediates from the previous cycle, which can block the active sites on the photocatalyst.[8] The weight of the W-TiEPS did not change during the reuse experiments.

4. Conclusions

EPS–TiO_2 composite was synthesized as a floating photocatalyst using a novel simple method, in which a diluted solvent was used. The TiO_2 particles were successfully immobilized on the surface of the EPS with a diluted solvent containing 10% (v/v) acetone and 4% (w/v) TiO_2. Various solvents that are capable of dissolving EPS, such as ethyl acetate and benzene, can also be used in the same manner. The photocatalytic efficiency to oxidize MB dye was maintained over 20 reuse cycles, with minimum TiO_2 leaching into the treated water. The floating photocatalyst was also very effective for photocatalytic reduction of Cr(VI) in industrial wastewater when amended with citric acid (as electron donor) under UV-A irradiation. Overall, proof of concept was offered that this facile (and scalable) diluted solvent preparation method can be used to recycle abundant waste EPS and produce floating photocatalysts. These preliminary results encourage future research to assess the merits and limitations of floating photocatalysts produced in this manner to oxidize or reduce photocatalytically various water and wastewater contaminants.

Conflicts of interest

There are no conflicts to declare.

Acknowledgements

This work was supported by the National Research Foundation (NRF) of Korea [Grant no. NRF-2018R1C1B5044937]. Partial funding for PJA was provided by the NSF ERC for Nanotechnology-Enabled Water Treatment (EEC-1449500).

References

1 A. Fujishima and K. Honda, *Nature*, 1972, **238**, 37–38.
2 J. A. Khan, M. Sayed, N. S. Shah, S. Khan, Y. Zhang, G. Boczkaj, H. M. Khan and D. D. Dionysiou, *Appl. Catal., B*, 2020, **265**, 118557.
3 T. Wang, S. Liu, W. Mao, Y. Bai, K. Chiang, K. Shah and J. Paz-Ferreiro, *J. Hazard. Mater.*, 2020, **389**, 121827.
4 W. W. Lai, M. H. Hsu and A. Y. Lin, *Water Res.*, 2017, **112**, 157–166.
5 X. Meng, W. Xu, Z. Li, J. Yang, J. Zhao, X. Zou, Y. Sun and Y. Dai, *Advanced Fiber Materials*, 2020, **2**, 93–104.
6 S. K. Loeb, P. J. J. Alvarez, J. A. Brame, E. L. Cates, W. Choi, J. Crittenden, D. D. Dionysiou, Q. Li, G. Li-Puma, X. Quan, D. L. Sedlak, T. David Waite, P. Westerhoff and J. H. Kim, *Environ. Sci. Technol.*, 2019, **53**, 2937–2947.
7 L. Yao, Z. Chen, J. Li and C. Shi, *J. Mol. Liq.*, 2020, **314**, 113613.
8 M. Murugalakshmi, G. Mamba and V. Muthuraj, *Appl. Surf. Sci.*, 2020, **527**, 146890.
9 C. G. Lee, H. Javed, D. Zhang, J. H. Kim, P. Westerhoff, Q. Li and P. J. J. Alvarez, *Environ. Sci. Technol.*, 2018, **52**, 4285–4293.

10 F. C. Kent, K. R. Montreuil, R. M. Brookman, R. Sanderson, J. R. Dahn and G. A. Gagnon, *Water Res.*, 2011, **45**, 6173–6180.
11 G. Duoerkun, Y. Zhang, Z. Shi, X. Shen, W. Cao, T. Liu, J. Liu, Q. Chen and L. Zhang, *Advanced Fiber Materials*, 2020, **2**, 13–23.
12 F. Magalhães and R. M. Lago, *Sol. Energy*, 2009, **83**, 1521–1526.
13 Z. Xing, J. Zhang, J. Cui, J. Yin, T. Zhao, J. Kuang, Z. Xiu, N. Wan and W. Zhou, *Appl. Catal., B*, 2018, **225**, 452–467.
14 M. Sboui, M. F. Nsib, A. Rayes, M. Swaminathan and A. Houas, *J. Environ. Sci.*, 2017, **60**, 3–13.
15 M. Dlugosz, P. Zmudzki, A. Kwiecien, K. Szczubialka, J. Krzek and M. Nowakowska, *J. Hazard. Mater.*, 2015, **298**, 146–153.
16 L. Wang, X. Wang, S. Cui, X. Fan, B. Zu and C. Wang, *Catal. Today*, 2013, **216**, 95–103.
17 C. Shifu and C. Gengyu, *Sol. Energy*, 2005, **79**, 1–9.
18 X. Wang, X. Wang, J. Zhao, J. Song, L. Zhou, J. Wang, X. Tong and Y. Chen, *Appl. Catal., B*, 2017, **206**, 479–489.
19 F. Magalhães, F. C. C. Moura and R. M. Lago, *Desalination*, 2011, **276**, 266–271.
20 S. Singh, H. Mahalingam and P. K. Singh, *Appl. Catal., A*, 2013, **462**, 178–195.
21 S. Chen, J. Ai, J. Chen, J. Lin and Q. Chen, *J. Appl. Polym. Sci.*, 2020, **137**, 48691.
22 C. A. De León-Condés, G. Roa-Morales, G. Martínez-Barrera, P. Balderas-Hernández, C. Menchaca-Campos and F. Ureña-Núñez, *J. Environ. Chem. Eng.*, 2019, **7**, 102841.
23 İ. Altın and M. Sökmen, *Appl. Catal., B*, 2014, **144**, 694–701.
24 S. Varnagiris, M. Urbonavicius, S. Sakalauskaite, R. Daugelavicius, L. Pranevicius, M. Lelis and D. Milcius, *Sci. Total Environ.*, 2020, **720**, 137600.
25 N. H. Ramli Sulong, S. A. S. Mustapa and M. K. Abdul Rashid, *J. Appl. Polym. Sci.*, 2019, **136**, 47529.
26 M. Jang, W. J. Shim, G. M. Han, M. Rani, Y. K. Song and S. H. Hong, *Environ. Pollut.*, 2017, **231**, 785–794.
27 S. Varnagiris, M. Urbonavicius, S. Tuckute, M. Lelis and D. Milcius, *Vacuum*, 2017, **143**, 28–35.
28 G. Johanson, *Patty's Toxicol.*, 2012, 735–752.
29 G. Wypych, *Handbook of polymers*, Elsevier, 2016.
30 C. Bawn and M. Wajid, *Trans. Faraday Soc.*, 1956, **52**, 1658–1664.
31 S. Cheng and G. S. Grest, *ACS Macro Lett.*, 2016, **5**, 694–698.
32 M. Sokmen, I. Tatlidil, C. Breen, F. Clegg, C. K. Buruk, T. Sivlim and S. Akkan, *J. Hazard. Mater.*, 2011, **187**, 199–205.
33 H. Su, Q. Li and T. Tan, *J. Chem. Technol. Biotechnol.*, 2006, **81**, 1797–1802.
34 L. Caballero, K. A. Whitehead, N. S. Allen and J. Verran, *J. Photochem. Photobiol., A*, 2009, **202**, 92–98.
35 Z. Wang, S. Jiang and H. Sun, *Iran. Polym. J.*, 2016, **26**, 71–79.
36 O. O. Ayeleru, S. Dlova, O. J. Akinribide, O. F. Olorundare, R. Akbarzadeh, D. M. Kempaiah, C. Hall, F. Ntuli, W. K. Kupolati and P. A. Olubambi, *Inorg. Chem. Commun.*, 2020, **113**, 107704.
37 H. Veisi, S. A. Mirshokraie and H. Ahmadian, *Int. J. Biol. Macromol.*, 2018, **108**, 419–425.
38 K. T. Drisya, M. Solis-Lopez, J. J. Rios-Ramirez, J. C. Duran-Alvarez, A. Rousseau, S. Velumani, R. Asomoza, A. Kassiba, A. Jantrania and H. Castaneda, *Sci. Rep.*, 2020, **10**, 13507.
39 S. Umamaheswari and M. Murali, *Chem. Eng.*, 2013, **64**, 19159–19164.
40 D. H. Y. Yanto, N. P. R. A. Krishanti, F. C. Ardiati, S. H. Anita, I. K. Nugraha, F. P. Sari, R. P. B. Laksana, S. Sapardi and T. Watanabe, *IOP Conf. Ser. Earth Environ. Sci.*, 2019, **308**, 012001.
41 S. B. Eskander and M. E. Tawfik, *Polym. Compos.*, 2011, **32**, 1430–1438.
42 J. A. Abdullah, A. G. Al Lafi, Y. Amin and T. Alnama, *Appl. Radiat. Isot.*, 2018, **136**, 73–81.
43 A. A. Ashkarran, M. Fakhari, H. Hamidinezhad, H. Haddadi and M. R. Nourani, *J. Mater. Res. Technol.*, 2015, **4**, 126–132.
44 M. Tasbihi, I. Călin, A. Šuligoj, M. Fanetti and U. Lavrenčič Štangar, *J. Photochem. Photobiol., A*, 2017, **336**, 89–97.
45 L. Zhang, Z. Xing, H. Zhang, Z. Li, X. Zhang, Y. Zhang, L. Li and W. Zhou, *ChemPlusChem*, 2015, **80**, 623–629.
46 J. Suave, S. M. Amorim and R. F. P. M. Moreira, *J. Environ. Chem. Eng.*, 2017, **5**, 3215–3223.
47 S. Wu, S. Zhang, Y. Gong, L. Shi and B. Zhou, *J. Hazard. Mater.*, 2020, **382**, 121045.
48 M. R. Samarghandi, J. K. Yang, O. Giahi and M. Shirzad-Siboni, *Environ. Technol.*, 2015, **36**, 1132–1140.
49 B. A. Marinho, R. O. Cristóvão, R. Djellabi, J. M. Loureiro, R. A. R. Boaventura and V. J. P. Vilar, *Appl. Catal., B*, 2017, **203**, 18–30.
50 L. Yang, Y. Xiao, S. Liu, Y. Li, Q. Cai, S. Luo and G. Zeng, *Appl. Catal., B*, 2010, **94**, 142–149.
51 B. A. Marinho, R. Djellabi, R. O. Cristóvão, J. M. Loureiro, R. A. R. Boaventura, M. M. Dias, J. C. B. Lopes and V. J. P. Vilar, *Chem. Eng. J.*, 2017, **318**, 76–88.
52 A. Mohamed, T. A. Osman, M. S. Toprak, M. Muhammed, E. Yilmaz and A. Uheida, *J. Mol. Catal. A: Chem.*, 2016, **424**, 45–53.
53 S. S. Emadian, M. Ghorbani and G. Bakeri, *Synth. Met.*, 2020, **267**, 116470.
54 M. Abinaya, K. Govindan, M. Kalpana, K. Saravanakumar, S. L. Prabavathi, V. Muthuraj and A. Jang, *J. Hazard. Mater.*, 2020, **397**, 122885.
55 D. Lu, W. Chai, M. Yang, P. Fang, W. Wu, B. Zhao, R. Xiong and H. Wang, *Appl. Catal., B*, 2016, **190**, 44–65.

